

Bootstrap percolation on spatial networks

Jian Gao¹, Tao Zhou^{1,2} and Yanqing Hu³

¹ Complx Lab, Web Sciences Center, University of Electronic Science and Technology of China, Chengdu 611731, People's Republic of China

² Big Data Research Center, University of Electronic Science and Technology of China, Chengdu 611731, People's Republic of China

³ School of Mathematics, Southwest Jiaotong University, Chengdu 610031, People's Republic of China

E-mail: yanqing.hu.sc@gmail.com (corresponding author)

Abstract. Bootstrap percolation can be essentially seen as a networked activation process and it has found applications in modeling phenomena on social networks, such as spreading of information and adoption of behaviors. In this paper, we study bootstrap percolation on spatial networks, in which the probability density function of a node to have a long-range link at distance r scales as $P(r) \sim r^\alpha$, where α is a tunable exponent. Setting the size of the giant active component as the order parameter, we find a parameter-dependent critical value α_c , above which a double phase transition is present. Here the so-called double phase transition means a mixture of two transitions, namely, a second-order phase transition at a smaller critical point and a hybrid phase transition at a larger critical point. In particular, $\alpha_c^* \approx -1$ is found to be a parameter-independent critical value, about which the two critical points for the double phase transition are almost constant. When $\alpha_c \leq \alpha < \alpha_c^*$, the first-order critical point decreases and the second-order critical point increases as α decreases. When $\alpha < \alpha_c$, the hybrid phase transition vanishes and there is only a second-order phase transition with an increasing critical point as the decreasing of α . As the scaling law $\alpha \approx -1$ has been well justified by many empirical studies of real online social networks, our results expand the current understanding on the spreading of information and the adoption of behaviors on spatial social networks.

PACS numbers: 89.75.Hc 64.60.ah 05.70.Fh

Keywords: bootstrap percolation, spatial networks, phase transition

1. Introduction

Bootstrap percolation was originally introduced by Chalupa, Leath and Reich [1] in the context of magnetic disordered systems in 1979. Since then, it has been studied extensively by physicists and sociologists, mainly due to its connections with various physical models and a variety of applications such as neuronal activity [2, 3] and jamming transitions [4, 5]. Bootstrap percolation can be essentially considered as an activation process on networks: (i) Nodes are either active or inactive; (ii) Once activated, a node remains active forever; (iii) Initially, each node is in an active state with a given probability p ; (iv) Subsequently, inactive nodes become active if they have at least k active neighbors; (v) Nodes are activated in an iterative manner according to the condition in (iv), until no more nodes can be activated. This process has been investigated on different kinds of networks including lattices [6, 7, 8, 9], trees [10, 11, 12], random networks [13, 14, 15, 16, 17], and so on.

Bootstrap percolation has found applications in modeling the spreading of information [18], the propagation of infection [19], the adoption of new products and social behaviors [20, 21, 22, 23] such as trends, fads, political opinions, belief, rumors, innovations and financial decisions. For instance, one may decide to buy a product when recommended by at least k users and trust a message when told by at least k neighbors; cf. the well-known rule, “What I tell you three times is true” [24]. In this way, the process leads initially localized effects propagating throughout the whole network. Moreover, a broad range of generalized formulations of bootstrap percolation on social networks are investigated, such as Watts’ model of opinions [25], in which k is replaced by a certain fraction of the neighbors, and disease transmission models with different degrees of severity of infection [26].

Real networks are often embedded in space [27] and social networks are no exception. Previous empirical studies of online social networks [28], email networks [29] and mobile phone communication networks [30] have confirmed a spatial scaling law, namely, the probability density function (PDF) of an individual to have a friend at distance r scales as $P(r) \sim r^\alpha$, $\alpha \approx -1$ [31]. In fact, prior to these empirical observations, Kleinberg [32] has proposed a spatial network model by adding long-range links to a 2-dimensional lattice, and he has proved that when $P(r) \sim r^{-1}$, the structure is optimal for information navigation. Recently, Hu *et al.* [31] suggested the optimization of information collection as a possible explanation for the origin of this spatial scaling law.

Extensive studies have shown that the spatial organization can change the dimension [33, 34, 35, 36], which dominates many important physical properties of networks [37, 38, 39, 40, 41]. Moukarzel *et al* [42] studied k-core percolation on long-range spatial networks, which is built by taking a 2-dimensional lattice and adding to each node one or more long-range links. In the networks, the probability density function (PDF) of long-range links with length r scales as $P(r) \sim r^\alpha$. By numerical simulation, they found that the 3-core transition is of first-order for $\alpha > -1.75$ (it is equivalent to the scaling of 2.75 in Ref [42]) and of second-order for smaller α . In fact, k-core percolation has close relation to bootstrap percolation [43, 44], nevertheless the two processes have different features from each other, being strongly dependent on the network structure [13, 45]. Although there is a deeper understanding

of percolation processes and spatial networks now, how spatial organization influences the spreading process on social networks under the framework of bootstrap percolation remains further investigation.

In this paper, we numerically study bootstrap percolation on undirected Kleinberg's spatial networks, which is a typical artificial social network. Setting the relative size of the giant active component to the network size as the order parameter, we find the distribution of long-range links' lengths can change the order of phase transition. In particular, we find a parameter-dependent critical value α_c , above which a double phase transition [46] is observed. Here, the so-called double phase transition means a mixture of two transitions at different critical points, consisting of a hybrid phase transition and a second-order one. In this paper, we use the hybrid phase transition to indicate a first-order phase transition in which the order parameter has a discontinuous jump between two non-zero values. Surprisingly, we find a parameter-independent critical value $\alpha_c^* \approx -1$, about which the two critical points for the double phase transition are almost constant. When $\alpha_c \leq \alpha < \alpha_c^*$, the first-order critical point decreases and the second-order critical point increases as α decreases. When $\alpha < \alpha_c$, there is only a second-order phase transition with an increasing critical point as the decreasing of α . Furthermore, we test the universality of our findings by drawing the phase diagram and give a possible explanation of the rich phase transition phenomena by simulating on related networks. Our findings indicate that the spatial scaling $\alpha \approx -1$, observed in real social networks, may be resulted from some deep-going principles in addition to the optimization of navigation and information collection, which is not yet fully understood now.

2. Model

Kleinberg model [32] is a typical spatial network model, which has been well justified by empirical data [28, 29, 30]. In this paper, the undirected Kleinberg's spatial network is constrained on a 2-dimensional periodic square lattice consisting of $N = L \times L$ nodes. In addition to its initially connected four nearest neighbors, each node i has a random long-range link to a node j with probability $Q_i(r_{ij}) \sim r_{ij}^{\alpha-1}$, where α is a tunable exponent and r_{ij} denotes the Manhattan distance, which quantifies the length of the shortest path between node i and node j , following strictly the horizontal and/or vertical links in lattices. Since the number of nodes at distance r to a given node is proportional to r^{d-1} in a d -dimensional lattice, the probability $Q(r_{ij})$ can be mapped to a probability density function (PDF), $P(r) \sim r^{d-1} \cdot Q(r) = r^{d-1} \cdot r^{\alpha-1} = r^{\alpha+d-2}$. In the present 2-dimensional case, where $d = 2$, the PDF scales as $P(r) \sim r^\alpha$. An illustration of a 2-dimensional undirected Kleinberg's spatial network can be found in figure 1.

In order to numerically implement the spatial scaling α when generating Kleinberg's spatial networks, we add undirected long-range links to a 2-dimensional periodic square lattice in a smart way as follows. First, a random length r between 2 and $L/2$ is generated with probability $P(r) \sim r^\alpha$, which ensures the scaling in advance. Second, random segmentations of length r to Δx and Δy with the only constraint that $|\Delta x| + |\Delta y| = r$ are done to determine candidate nodes, where Δx and Δy are both integers. Namely, for an uncoupled node i

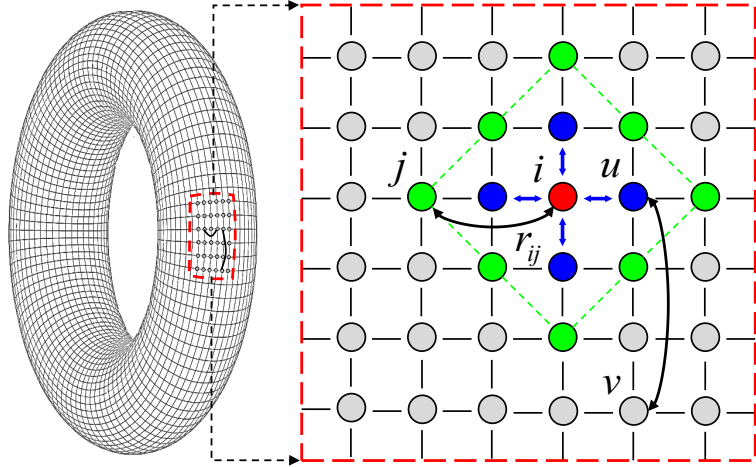


Figure 1. An illustration of an undirected Kleinberg's spatial network constrained on a 2-dimensional periodic square lattice. Each node has four short-range links (colored blue for node i) and one long-range link (colored black). The probability density function (PDF) of a node to have a long-range link at Manhattan distance r scales as $P(r) \sim r^\alpha$. For the target node i (colored red), when $r = 2$, there are eight candidate nodes (colored green), from which we can choose an uncoupled node j to make a connection. For another target node u , we can choose to connect it with node v when $r = 3$.

with coordinates (x, y) , named target node, all candidate nodes are these with coordinates $(x + \Delta x, y + \Delta y)$ such that $|\Delta x| + |\Delta y| = r$. The above procedure ensures all candidate nodes at distance r from the target node i are uniformly distributed. Hence, we can randomly choose an uncoupled candidate node (i.e., a node without any long-range link) to link with target node i . Be noted that, on a large system, a finite fraction of the nodes will have all candidate nodes already connected when α is very small. To deal with this problem, we additionally adopt an alternate procedure referring to the distance coarse graining procedure [47], in which we randomly choose an uncoupled nearest neighbor node of these candidate nodes until the linking is accomplished. We repeat such procedure for the rest uncoupled nodes until each node of the network has one undirected long-range link such that the degree of each node is exactly 5.

3. Results

We focus on the following three indicators: (i) The relative size of the giant active component (S_{gc}) at the equilibrium, i.e., the probability that an randomly selected node belongs to the giant active component; (ii) The number of iterations (NOI) to reach the equilibrium, which is usually used to determine the critical point for the first-order phase transition [48, 49]; (iii) The relative size of the second giant active component (S_{gc2}), which is usually used to determine the critical point for the second-order phase transition [35, 49].

Figure 2 shows rich phase transition phenomena when taking S_{gc} as the order parameter. When $\alpha \geq -1$, the curves of $S_{gc}(p)$ are well overlapped and the system undergoes a double

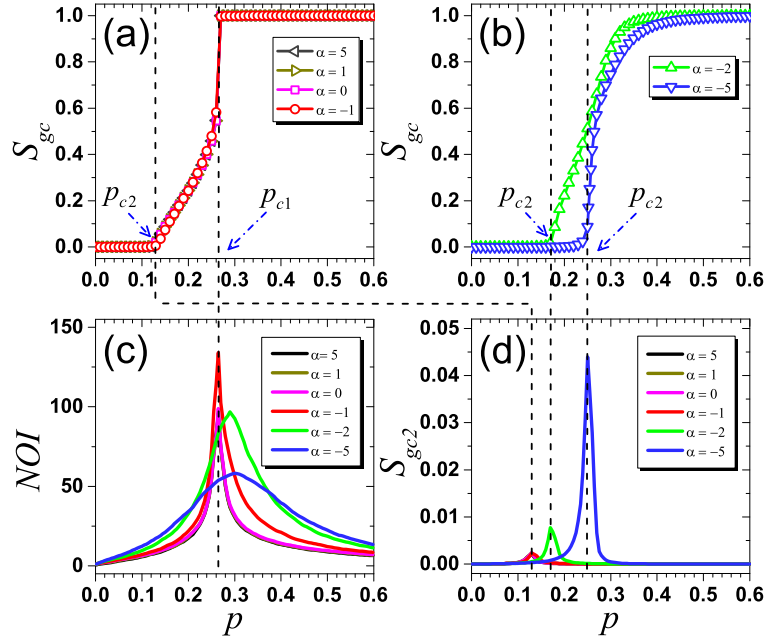


Figure 2. S_{gc} , NOI and S_{gc2} as a function of p for different α after $k = 3$ bootstrap percolation on undirected Kleinberg's spatial networks. Two different types of $S_{gc}(p)$ curves are observed, including a double phase transition (a) and a second-order one (b). When $\alpha \geq -1$, $S_{gc}(p)$ curves behave alike and a double phase transition is present. S_{gc} abruptly jumps to 1 at $p_{c1} \approx 0.263$, where NOI reaches its maximum (c). When $\alpha < -1$, there is only a second-order phase transition with an increasing critical point as the increasing of α , where S_{gc2} reaches its maximum at different p_{c2} (d). Dash lines mark identification of critical points. Results are obtained by simulations on networks with fixed size $L = 400$ and averaged over 1000 realizations.

phase transition, mixed of a hybrid phase transition and a second-order one as shown in figure 2(a). Notice that S_{gc} has a continuous increase at $p_{c2} \approx 0.134$ (the second-order critical point), where the transition is of second-order. In contrast, S_{gc} has an abrupt jump directly from around 0.58 to almost 1 at $p_{c1} \approx 0.263$ (the first-order critical point), where there is a hybrid phase transition. Surprisingly, the two critical points seem to be constant when $\alpha \geq -1$, as indicated by the four overlapped $S_{gc}(p)$ curves in figure 2(a). When $\alpha < -1$, there is only a second-order phase transition with an increasing p_{c2} as the decreasing of α (see figure 2(b)). Specifically, $p_{c2} \approx 0.176$ when $\alpha = -2$ and $p_{c2} \approx 0.256$ when $\alpha = -5$. Although S_{gc} goes up sharper after p exceeds p_{c2} as α getting smaller, simulations justify that the curve of $S_{gc}(p)$ is still continuous, meaning that the transition is indeed of second-order when $\alpha < -1$.

Finding critical points via simulations is always a difficult task that requires high precision. When $\alpha \geq -1$, where a part of the double phase transition is a hybrid phase transition, we can determine the critical point p_{c1} by calculating the number of iterations (NOI) in the cascading process, since NOI sharply increases when p approaches p_{c1} for the first-order phase transitions [48, 49]. Accordingly, p_{c1} is calculated by plotting NOI as a function of p . As shown in figure 2(c), NOI reaches its maximum at the same p when $\alpha \geq -1$, which is the evidence that $p_{c1} \approx 0.263$ is almost a constant value. Analogously, by

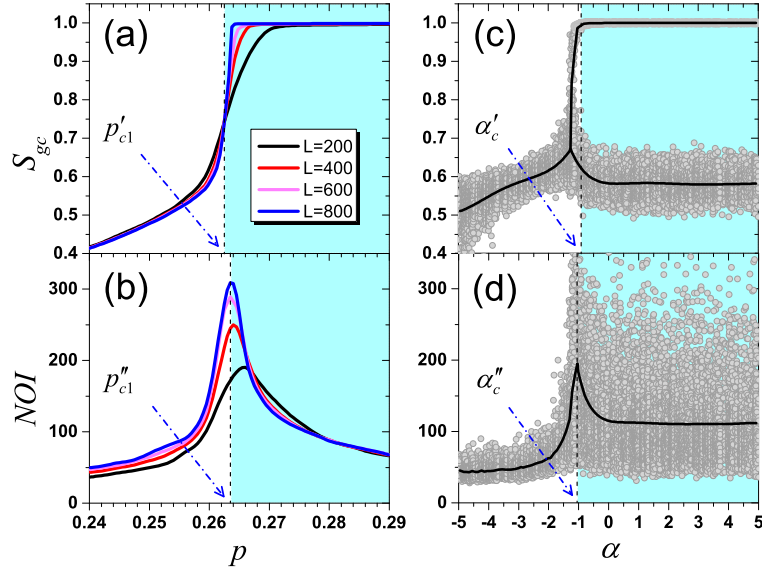


Figure 3. Cross-validation of p_{c1} and α_c . (a) and (b) are for S_{gc} and NOI under different network size L when $\alpha = -1$, respectively. There is an intersection of $S_{gc}(p)$ at $p'_{c1} \approx 0.2625$, while NOI reaches its maximum at $p''_{c1} \approx 0.2635$ when $L = 800$. Thus, p_{c1} is identified as the average value 0.263. (c) and (d) are S_{gc} and NOI when $p = 0.263$ under different α , respectively. For $\alpha > \alpha'_c \approx -0.95$, S_{gc} has two phases, and NOI reaches its maximum at $\alpha''_c \approx -1.05$. Thus, α_c is identified as the average value -1 . In (c) and (d), dark curves respectively represent the average values of S_{gc} and NOI , obtained from 1000 realizations, and each data point stands for one realization.

plotting S_{gc2} as a function of p , we can precisely identify p_{c2} [35, 49], at which S_{gc2} reaches its maximum (see figure 2(d)). We can see that p_{c2} increases as α decreases, as $p_{c2} \approx 0.134$ ($\alpha \geq -1$), 0.176 ($\alpha = -2$) and 0.256 ($\alpha = -5$).

Although to justify the hybrid phase transition and to determine the critical value α_c by simulations in a finite discrete system are not easy, we solve this problem by a cross-validation on the critical point p_{c1} and the critical value α_c . Firstly, we fix $\alpha = -1$ to determine p_{c1} . On the one hand, there is an intersection for curves of $S_{gc}(p)$ at $p'_{c1} \approx 0.2625$ under different network sizes as shown in figure 3(a), which can be considered as the critical point according to the finite-size analysis [49]. On the other hand, the corresponding NOI reaches its maximum at $p''_{c1} \approx 0.2635$ when $L = 800$ as shown in figure 3(b). Combining these two observations, a more appropriate critical point is identified as the average value $p_{c1} = (p'_{c1} + p''_{c1})/2 \approx 0.263$. Conversely, we fix $p = 0.263$ to determine α_c . From figure 3(c), we can see that S_{gc} has two phases: about 0.58 or close to 1 when $\alpha \geq \alpha'_c \approx -0.95$, which is a strong evidence that S_{gc} undergoes a hybrid phase transition. If the increasing of S_{gc} is continuous, there is no such gap between the two phases. From figure 3(d), we note that the corresponding averaging NOI reaches its maximum at $\alpha = \alpha''_c \approx -1.05$. Combining these two evidences, we appropriately identify the critical value as the average value $\alpha_c = (\alpha'_c + \alpha''_c)/2 \approx -1$.

In addition, p_{c1} for the hybrid phase transition should be almost constant when $\alpha \geq \alpha_c$,

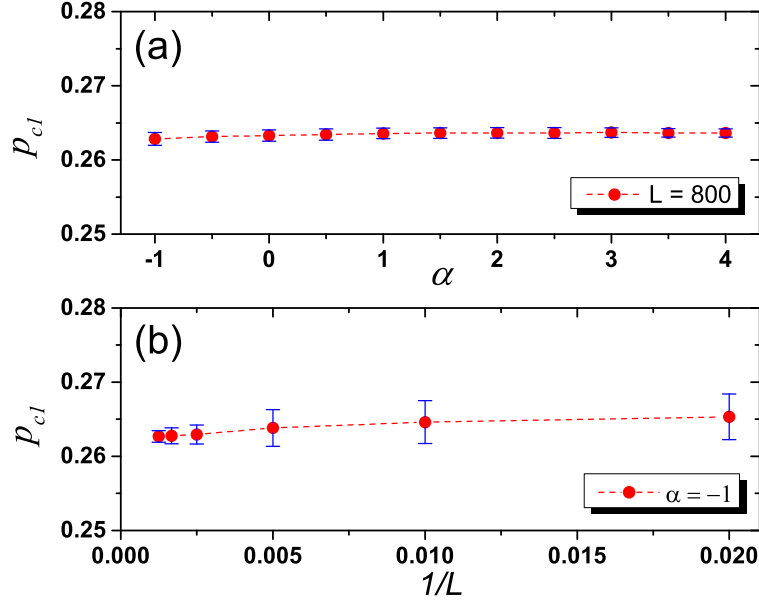


Figure 4. (a) Error estimation of p_{c1} with fixed network size $L = 800$. As α approaches the critical value -1 , p_{c1} slightly decreases, but being kept in a very narrow range. When α is in range $[-1, 4]$, the mean value of p_{c1} is 0.2634, and the difference between maximum and minimum value of p_{c1} is 0.0008. (b) Analysis on the effects of finite-size. The data point and the error bar are respectively mean value and standard deviation of the identified p_{c1} in the case of $\alpha = -1$ under different network sizes L . As L goes to infinity (from the right side to the left side in (b)), the mean value of p_{c1} gradually approaches an extreme value around 0.263, and the standard deviation of the p_{c1} decreases. Results are obtained by averaging over 1000 realizations.

otherwise we cannot observe the separation of two phases in figure 3(c) for a fixed value $p = 0.263$. To verify that, we estimate errors of p_{c1} by varying α under fixed network size L . As shown in figure 4(a), p_{c1} slightly decreases when α approaches the critical value $\alpha_c \approx -1$. Even though, when α is in the range $[-1, 4]$, the difference between maximum and minimum value of p_{c1} is only 0.0008 after over 1000 realizations, which is very small compared to the whole range of p (i.e. $[0, 1]$), indicating that the value of p_{c1} is not sensitive to the parameter α when $\alpha \geq -1$. Based on these evidences, p_{c1} can be roughly considered as a constant and its value is about 0.2634, which is the mean value of p_{c1} when α in the range $[-1, 4]$. Furthermore, taking $\alpha = -1$ as an example, we consider the effects of finite-size of networks on these results. As shown in figure 4(b), the mean value of p_{c1} gradually approaches an extreme value around 0.263, and the standard deviation of p_{c1} decreases as L goes to infinity. Similar results hold for the analysis of the critical point p_{c2} and its value is also almost constant as 0.134.

A representative phase diagram for S_{gc} in the $p - \alpha$ plane is shown in figure 5. We find that the varying of α , which dominates the distribution of long-range links' lengths, can change the order of phase transition. Overall, $\alpha_c \approx -1$ is confirmed to be a critical value, above which a double phase transition (region II) is present. When $\alpha \geq -1$, the curves of $S_{gc}(p)$ are overlapped, suggesting that the properties of bootstrap percolation on these

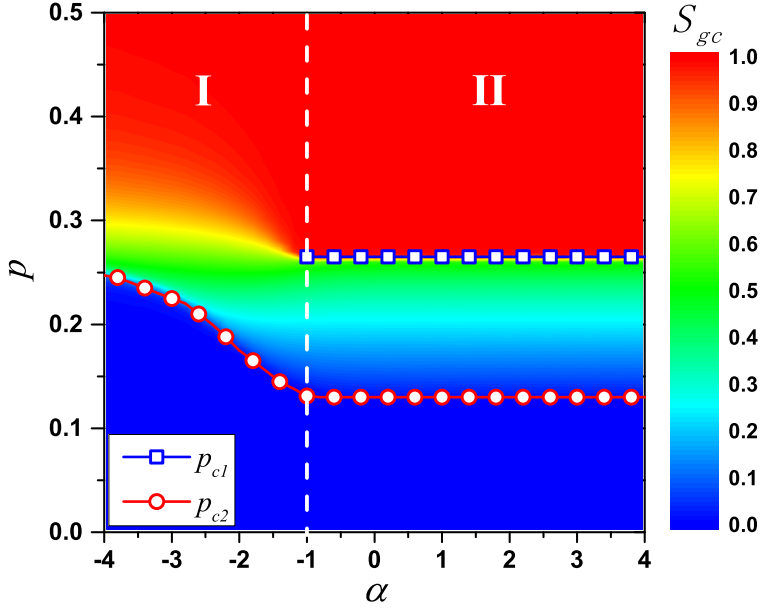


Figure 5. Phase diagram of $k = 3$ bootstrap percolation in the $p - \alpha$ plane. The color marks the value of S_{gc} . Dashed lines with solid squares and circles represent p_{c1} and p_{c2} , respectively. Separated by $\alpha = -1$, a double phase transition is observed in the right region II with two almost constant critical points $p_{c1} \approx 0.263$ and $p_{c2} \approx 0.134$. In the left region I, only a second-order phase transition is present with an increasing critical point as α decreases. The critical point is up to $p_{c2}^\infty \approx 0.259$, which is obtained in the case of all long-range links' lengths are 2. Results are averaged over 1000 realizations with fixed network size $L = 400$.

spatial networks are alike. When $\alpha < -1$, the hybrid phase transition vanishes and S_{gc} only undergoes a second-order phase transition (region I) with an increasing critical point as the decreasing of α . The maximum of p_{c2} is about 0.259, which is obtained when $\alpha \rightarrow -\infty$, i.e., all long-range links' lengths are 2.

To test the universality of our findings, we simulated on undirected Kleinberg's spatial networks in parameter spaces (k, α, k_l) and determined the corresponding critical points. As shown in figure 6, according to the relationship between the threshold k and half of the average degree of the network $\langle k_N \rangle / 2$, where $\langle k_N \rangle = k_l + 4$, there are three regions in the phase diagram:

- (i) When k is remarkably smaller than $\langle k_N \rangle / 2$, e.g., $k = 1$ compared to $\langle k_N \rangle / 2 = 2.5$, there is only a trivial first-order phase transition at $p_{c1} \approx 0$.
- (ii) When k is around $\langle k_N \rangle / 2$, e.g., $k = 3$ compared to $\langle k_N \rangle / 2 = 2.5$, there is a critical value α_c , above which a double phase transition is observed. The value of α_c depends on the choice of both k and k_l . In particular, $\alpha_c^* \approx -1$ is found to be a parameter-independent critical value, about which the two critical points for the double phase transition are almost constant. Specifically, as shown in the phase diagram of figure 6, the color of data points for the same parameter k is nearly unchanged when $\alpha \geq -1$, which is a strong evidence that the values of p_{c1} and p_{c2} are almost constant. When $\alpha_c \leq \alpha < \alpha_c^*$, p_{c1} decreases and p_{c2} increases as α decreases. Note that α_c can be equal to α_c^* in some

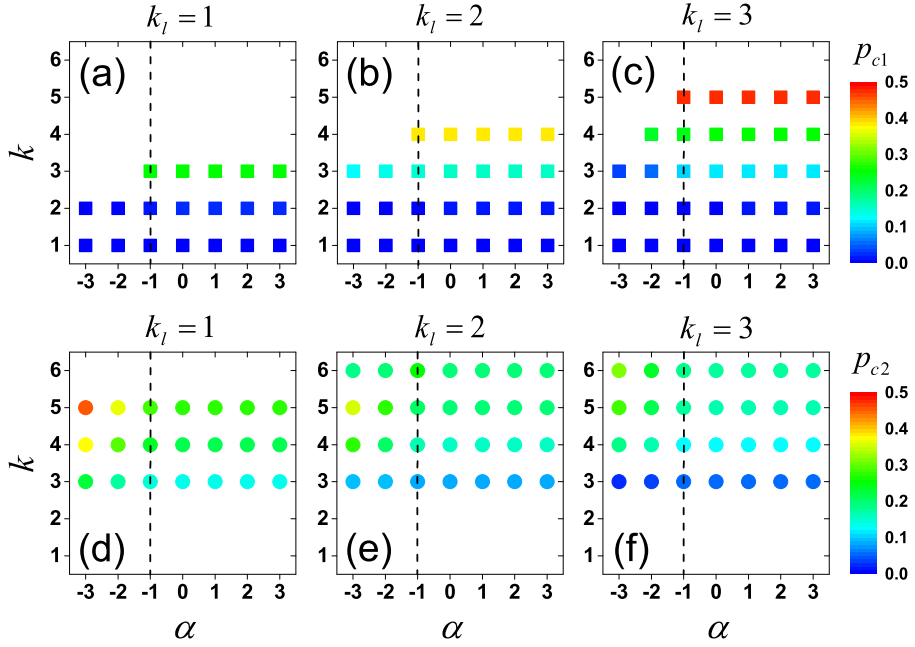


Figure 6. Phase diagram of bootstrap percolation on undirected Kleinberg’s spatial networks in parameter spaces (k, α, k_l) . The color of data points in (a), (b) and (c) marks the value of p_{c1} , where there is a hybrid phase transition (or a first-order phase transition in the trivial cases where $p_{c1} \approx 0$), and the color of data points in (d), (e) and (f) marks the value of p_{c2} , where the transition is of second-order. Blank areas stand for the absent of the corresponding phase transitions. Separated by the vertical dash line $\alpha = -1$, on the right side, the color of data points is nearly unchanged for the same parameter k , meaning that the values of p_{c1} and p_{c2} are almost invariant. $\alpha_c^* \approx -1$ is found to be a parameter-independent critical value, above which the critical points for the double phase transition are almost constant. When $\alpha_c \leq \alpha < \alpha_c^*$, p_{c1} decreases and p_{c2} increases as α decreases. When $\alpha < \alpha_c$, p_{c2} increases as α decreases. Results are averaged over 1000 realizations with fixed network size $L = 400$.

parameter spaces, such as $(k, k_l) = (3, 1)$ and $(k, k_l) = (4, 2)$.

- (iii) When k is remarkably larger than $\langle k_N \rangle / 2$, e.g., $k = 5$ compared to $\langle k_N \rangle / 2 = 2.5$, the hybrid phase transition is absent and S_{gc} only undergoes a second-order phase transition with an increasing p_{c2} as the decreasing of α (see figures S1-S3 of the supplementary information for the detailed shapes of $S_{gc}(p)$ curves).

Moreover, simulations confirm that our main results also hold for Kleinberg’s spatial networks with directed long-range links since $\alpha_c^* \approx -1$ is still a critical value. However, there is only a first-order phase transition with p_{c1} being almost constant instead of the formal double transition when $\alpha \geq -1$ (see figure S4 of the supplementary information). In addition, simulations on undirected Kleinberg’s spatial networks without periodic boundary conditions suggest that whether the square lattice has periodic boundary conditions does not essentially affect our main results (see figure S5 of the supplementary information).

To provide the insights on the mechanism of the transition, we simulate on different networks and compare with other related transitions. These networks include a simple 2-dimensional lattice (Lattice), networks with all 5 links being long-range (LR) and networks

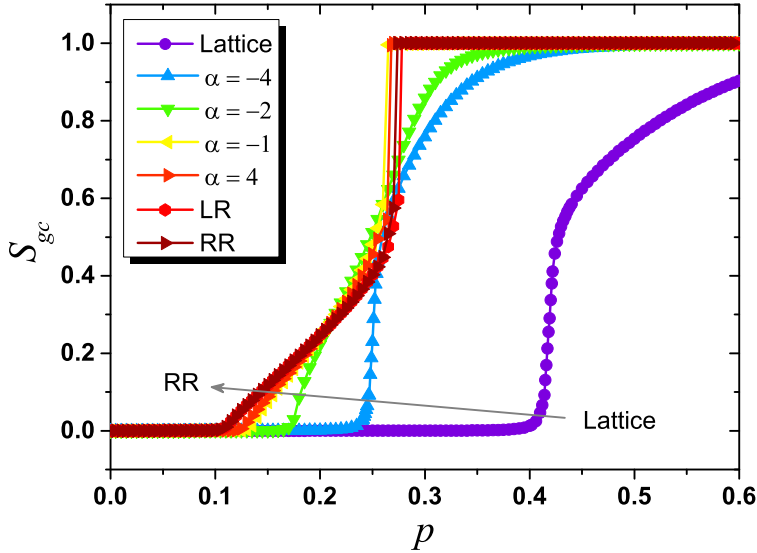


Figure 7. S_{gc} as a function of p after $k = 3$ bootstrap percolation on different networks, including Lattice, LR, RR and the present spatial networks with different α . When $\alpha = -4$, the curve of $S_{gc}(p)$ on the spatial network behaves like the one on Lattice network, and the transition is of second-order. As α increases, the transition turns into a double phase transition when $\alpha \geq -1$, where the curves of $S_{gc}(p)$ are almost overlapped with the ones on LR network and RR network. The parameter for LR network is set as $\alpha = -1$. Results are averaged over 1000 realizations with fixed network size $L = 400$

without spatial structure, i.e. random 5-regular networks (RR). In the LR network, which is a special case of long-range percolation model in the 2-dimensional space [50, 51, 52], each node is associated with only $k_l = 5$ undirected long-range links instead of initially connected short-range links based on a 2-dimensional periodic lattice. As shown in figure 7, the curves of $S_{gc}(p)$ on the spatial networks are between the ones on Lattice network and RR network. When $\alpha = -4$, the $S_{gc}(p)$ curve on the spatial network has similar trend with the one on Lattice network since the very long-range links are rare, and the transition is of second-order. When $\alpha \geq -1$, there is a double phase transition and the curves of $S_{gc}(p)$ are almost overlapped with the one on RR network. These observations indicate that, to turn the value of α , we can change the bootstrap percolation properties of spatial networks from Lattice network to RR network, or vice versa. More specifically, when $\alpha = -4$, all long-range links are highly localized and the structure of spatial networks is similar to Lattice network, whereas when $\alpha \geq -1$, mainly due to the existence of very long-range links, the spatial networks behave like RR network.

Together, it should be noted that the $S_{gc}(p)$ curve on LR network when $\alpha = -1$ acts like the ones on RR network and spatial networks when $\alpha \geq -1$. To better understand how does α affect the transition on LR network, taking $k_l = 5$ as an example, we show the phase diagram after $k = 3$ bootstrap percolation in figure 8. The diagram is divided into three regions by critical values $\alpha_c \approx -2$ and $\alpha_c^* \approx -1$. As α decreases, the transition is of second-order with an increasing p_{c2} when $\alpha < \alpha_c \approx -2$ (region I). There is a double phase transition when

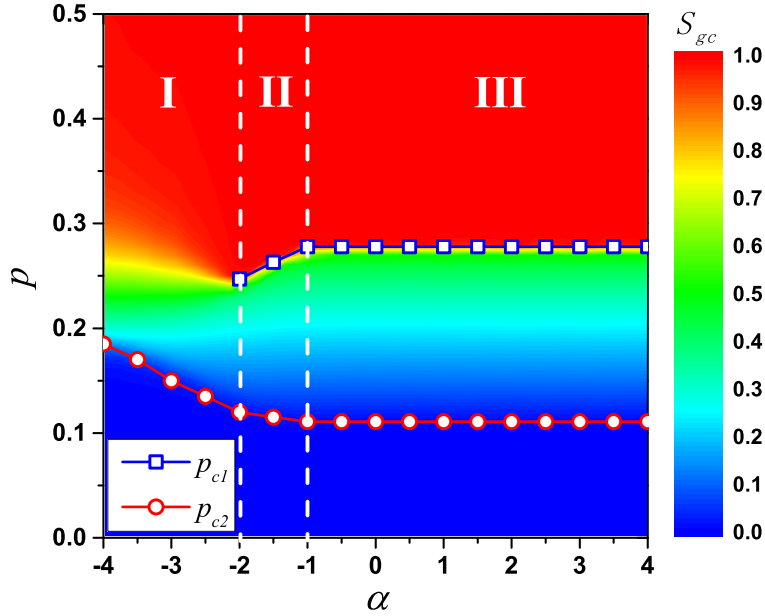


Figure 8. Phase diagram of $k = 3$ bootstrap percolation in the $p - \alpha$ plane on LR networks with $k_l = 5$. The color marks the value of S_{gc} . As α decreases, the transition is of second-order with an increasing p_{c2} in the region I where $\alpha < -2$. When α decreases, a double phase transition is observed in the region II where $-2 \leq \alpha < -1$, with a decreasing p_{c1} for the hybrid phase transition and an increasing p_{c2} for the second-order phase transition. In the region III where $\alpha \geq -1$, the double phase transition is with two almost constant critical points, $p_{c1} = 0.278$ and $p_{c2} = 0.111$. Results are averaged over 1000 realizations with fixed network size $L = 400$.

$\alpha_c \approx -2 \leq \alpha < \alpha_c^* \approx -1$ (region II), where p_{c1} decreases and p_{c2} increases as α decreases. Once again, a double phase transition with two almost constant critical points, $p_{c1} \approx 0.278$ and $p_{c2} \approx 0.111$, is observed when $\alpha \geq \alpha_c^* \approx -1$ (region III). Further simulations suggest that similar main results also hold under other combinations of k and k_l (see figures S4 for the phase diagram and S5-S9 for the shapes of $S_{gc}(p)$ curves in the supplementary information).

In fact, for the original Kleinberg's spatial networks with directed long-range links, Sen *et al* [53] found that the varying of α can change the network structure, namely, the network is regular-lattice-like when $\alpha < -2$, small-world-like when $-2 < \alpha < -1$ and random-like when $\alpha > -1$. More recent studies [33, 34, 35] also proposed three regimes: (i) When $\alpha > -1$, the dimension of the spatial network is $d = \infty$ and the percolation transition belongs to the university class of percolation in Erdős-Rényi networks. (ii) When $-3 < \alpha < -1$, d decreases continuously from $d = \infty$ to $d = 2$ and the percolation shows new intermediate behavior. (iii) When $\alpha < -3$, the dimension is $d = 2$ and the percolation transition belongs to the university class of percolation in regular lattices. These previous findings suggest that the properties of spatial networks have qualitative changes when α is around -1 , which is correspond to the observation of these phase transition phenomena here.

4. Conclusions and Discussion

We have studied bootstrap percolation on spatial networks, where the distribution patterns of long-range links' lengths can change the order of phase transition. In particular, we find a parameter-dependent critical value α_c , above which a double phase transition, mixed of a hybrid phase transition at a higher p and a second-order phase transition at a lower p , is present. It is particularly interesting that we find a almost parameter-independent critical value $\alpha_c^* \approx -1$, about which the curves of $S_{gc}(p)$ are well overlapped, indicating that the two critical points for the double phase transition are almost constant when $\alpha \geq -1$. Such results indicate that the topological properties of undirected Kleinberg's spatial networks are alike when $\alpha \geq -1$ in the 2-dimensional space. In fact, the scaling law $\alpha \approx -1$ has been empirically observed in many real networks [28, 29, 30], which may be resulted from complex self-organizing processes toward optimal structures for information collection [31] and/or navigation [32]. Since the cascading processes on spatial networks are almost the same when $\alpha \geq -1$, $\alpha \approx -1$ is indeed corresponding to the structure with the smallest average geographical length of links, which can exhibit as effective spreading of information as networks with even longer shortcut links. This is to some extent relevant to the principle of least effort in human behavior [54].

We find the varying of α can change the bootstrap percolation critical behavior from random regular networks to lattices, or vice versa. In particular, when $\alpha \geq \alpha_c^* \approx -1$, the spatial networks behave like random regular networks and there is a double phase transition. When $\alpha_c < \alpha_c^*$, there is a richer phase transition phenomena. More specifically, the double phase transition is still present when $\alpha_c \leq \alpha < \alpha_c^*$, however, instead of being constant, the first-order critical point decreases and the second-order critical point increases as α decreases. The observation of such results may be mainly due to the small-world-like network structure [53, 55], which leads the transition showing a intermediate behavior. When $\alpha < \alpha_c$, the hybrid phase transition vanishes and there is only a second-order phase transition with an increasing critical point as the decreasing of α . When α goes to negative infinity, where all long-range links are highly localized, the spatial networks degenerates into regular lattices and the transition is of second-order. In this way, we give a possible explanation of the emergence of these phase transition phenomena.

Moreover, our results are, to some extent, relevant to the control of information spreading. For example, when $\alpha \geq \alpha_c$, if we would like to make as many people as possible to know the information, the optimal choice of the fraction of initially informed people should be p_{c1} , since larger initially informed population provides no more benefit but requires higher cost as shown in figure 2(a). However, in the context of a numerical study, it is really hard to tell whether the critical value α_c^* is exactly -1 and whether the critical points are completely independent of α when $\alpha \geq \alpha_c^*$. In addition, how does the transition depend on the spreading processes and what kind of transitions does it belong to for real social networks are still open questions. Hence, we expect to verify our findings in an analytical way and based on other network models, including spatially constrained Erdős-Rényi networks [56], multiplex networks [57, 58] and real social networks. Besides, to assign each node one long-range link is

a high-cost strategy when generating artificial spatial social networks, we leave individualized number of long-range links associated with each node and partial spatial embedding as future works.

Acknowledgments

We acknowledge the anonymous referees for their valuable comments and constructive suggestions. We thank Jun Wang and Panhua Huang for useful discussions. This work is partially supported by National Natural Science Foundation of China under Grants Nos. 61203156 and 11222543. J.G. acknowledges support from Tang Lixin Education Development Foundation by UESTC. T.Z. acknowledges the Program for New Century Excellent Talents in University under Grant No. NCET-11-0070, and Special Project of Sichuan Youth Science and Technology Innovation Research Team under Grant No. 2013TD0006.

References

- [1] Chalupa J, Leath P L and Reich G R 1979 *J. Phys. C: Solid State Phys.* **12** L31
- [2] Soriano J, Martínez M R, Tlusty T and Moses E 2008 *Proc. Natl. Acad. Sci. USA* **105** 13758–63
- [3] Goltsev A V, De Abreu F V, Dorogovtsev S N and Mendes J F F 2010 *Phys. Rev. E* **81** 061921
- [4] De Gregorio P, Lawlor A, Bradley P and Dawson K A 2005 *Proc. Natl. Acad. Sci. USA* **102** 5669–73
- [5] Toninelli C, Biroli G and Fisher D S 2006 *Phys. Rev. Lett.* **96** 035702
- [6] Kogut P M and Leath P L 1981 *J. Phys. C: Solid State Phys.* **14** 3187
- [7] Holroyd A E 2003 *Probab. Theory Relat. Fields* **125** 195–224
- [8] Gravner J, Holroyd A and Morris R 2012 *Probab. Theory Relat. Fields* **153** 1–23
- [9] Sausset F, Toninelli C, Biroli G and Tarjus G 2010 *J. Stat. Phys.* **138** 411–30
- [10] Balogh J, Peres Y and Pete G 2006 *Combin. Probab. Comput.* **15** 715–30
- [11] Biskup M and Schonmann R 2009 *J. Stat. Phys.* **136** 667–76
- [12] Bollobás B, Gunderson K, Holmgren C, Janson S and Przykucki M 2014 *Electron. J. Probab.* **19** 1–27
- [13] Baxter G J, Dorogovtsev S N, Goltsev A V and Mendes J F F 2010 *Phys. Rev. E* **82** 011103
- [14] Balogh J and Pittel B G 2007 *Random Struct. Algorithms* **30** 257–86
- [15] Janson S, Łuczak T, Turova T and Vallier T 2012 *Ann. Appl. Probab.* **22** 1989–2047
- [16] Amini H and Fountoulakis N 2014 *J. Stat. Phys.* **155** 72–92
- [17] Wu C, Ji S, Zhang R, Chen L, Chen J, Li X and Hu Y 2014 *Europhys. Lett.* **107** 48001
- [18] Shrestha M and Moore C 2014 *Phys. Rev. E* **89** 022805
- [19] Bizhani G, Paczuski M and Grassberger P 2012 *Phys. Rev. E* **86** 011128
- [20] Bradonjić M and Saniee I 2014 *Probab. Eng. Inform. Sc.* **28** 169–81
- [21] Ree S 2012 *Phys. Rev. E* **85** 045101
- [22] Centola D 2010 *Science* **329** 1194–7
- [23] Lü L, Chen D B and Zhou T 2011 *New J. Phys.* **13** 123005
- [24] Carroll L 1876 *The Hunting of the Snark* (London: Macmillan)
- [25] Watts D J 2002 *Proc. Natl. Acad. Sci. USA* **99** 5766–71
- [26] Ball F and Britton T 2009 *Math. Biosci.* **218** 105–20
- [27] Barthélémy M 2011 *Phys. Rep.* **499** 1–101
- [28] Liben-Nowell D, Novak J, Kumar R, Raghavan P and Tomkins A 2005 *Proc. Natl. Acad. Sci. USA* **102** 11623–8
- [29] Adamic L and Adar E 2005 *Soc. Networks* **27** 187–203

- [30] Lambiotte R, Blondel V D, de Kerchove C, Huens E, Prieur C, Smoreda Z and Van Dooren P 2008 *Physica A* **387** 5317–25
- [31] Hu Y, Wang Y, Li D, Havlin S and Di Z 2011 *Phys. Rev. Lett.* **106** 108701
- [32] Kleinberg J M 2000 *Nature* **406** 845
- [33] Emmerich T, Bunde A, Havlin S, Li G and Li D 2013 *Phys. Rev. E* **87** 032802
- [34] Kosmidis K, Havlin S and Bunde A 2008 *Europhys. Lett.* **82** 48005
- [35] Li D, Li G, Kosmidis K, Stanley H, Bunde A and Havlin S 2011 *Europhys. Lett.* **93** 68004
- [36] Li D, Kosmidis K, Bunde A and Havlin S 2011 *Nat. Phys.* **7** 481–4
- [37] Moukarzel C F 2005 *Physica A* **356** 157–61
- [38] Shekhtman L M, Berezin Y, Danziger M M and Havlin S 2014 *Phys. Rev. E* **90** 012809
- [39] Huang W, Chen S and Wang W 2014 *Physica A* **393** 132–54
- [40] Xie Y B, Zhou T, Bai W J, Chen G, Xiao W K and Wang B H 2007 *Phys. Rev. E* **75** 036106
- [41] Feng L, Monterola C P and Hu Y 2015 arXiv:1502.01601
- [42] Moukarzel C F and Sokolowski T 2010 *J. Phys.: Conf. Ser.* **246** 012019
- [43] Dorogovtsev S N, Goltsev A V and Mendes J F F 2006 *Phys. Rev. Lett.* **96** 040601
- [44] Goltsev A V, Dorogovtsev S N and Mendes J F F 2006 *Phys. Rev. E* **73** 056101
- [45] Baxter G J, Dorogovtsev S N, Goltsev A V and Mendes, J F F 2011 *Phys. Rev. E* **83** 051134
- [46] Colomer-de-Simón P and Boguñá M 2014 *Phys. Rev. X* **4** 041020
- [47] Zeng A, Zhou D, Hu Y, Fan Y and Di Z 2011 *Physica A* **390** 3962–9
- [48] Parshani R, Buldyrev S V and Havlin S 2011 *Proc. Natl. Acad. Sci. USA* **108** 1007–10
- [49] Liu R R, Wang W X, Lai Y C and Wang B H 2012 *Phys. Rev. E* **85** 026110
- [50] Schulman L S 1983 *J. Phys. A: Math. Gen.* **16** L639
- [51] Newman C M and Schulman L S 1986 *Commun. Math. Phys.* **104** 547–71
- [52] Benjamini I and Berger N 2001 *Random Struct. Algorithms* **19** 102–11
- [53] Sen P, Banerjee K and Biswas T 2002 *Phys. Rev. E* **66** 037102
- [54] Zipf G K 1949 *Human behavior and the principle of least effort* (Oxford: Oxford Press)
- [55] Watts D J and Strogatz S H 1998 *Nature* **393** 440–2
- [56] Schmeltzer C, Soriano J, Sokolov I M and Rüdiger S 2014 *Phys. Rev. E* **89** 012116
- [57] Baxter G J, Dorogovtsev S N, Mendes J F F and Cellai D 2014 *Phys. Rev. E* **89** 042801
- [58] Azimi-Tafreshi N, Dorogovtsev S N and Mendes J F F 2014 *Phys. Rev. E* **90** 052809

Bootstrap percolation on spatial networks

Jian Gao¹, Tao Zhou^{1,2} and Yanqing Hu³

¹ CompeX Lab, Web Sciences Center, University of Electronic Science and Technology of China, Chengdu 611731, People's Republic of China

² Big Data Research Center, University of Electronic Science and Technology of China, Chengdu 611731, People's Republic of China

³ School of Mathematics, Southwest Jiaotong University, Chengdu 610031, People's Republic of China

E-mail: yanqing.hu.sc@gmail.com (corresponding author)

Supplementary Information

1. S_{gc} for spatial networks

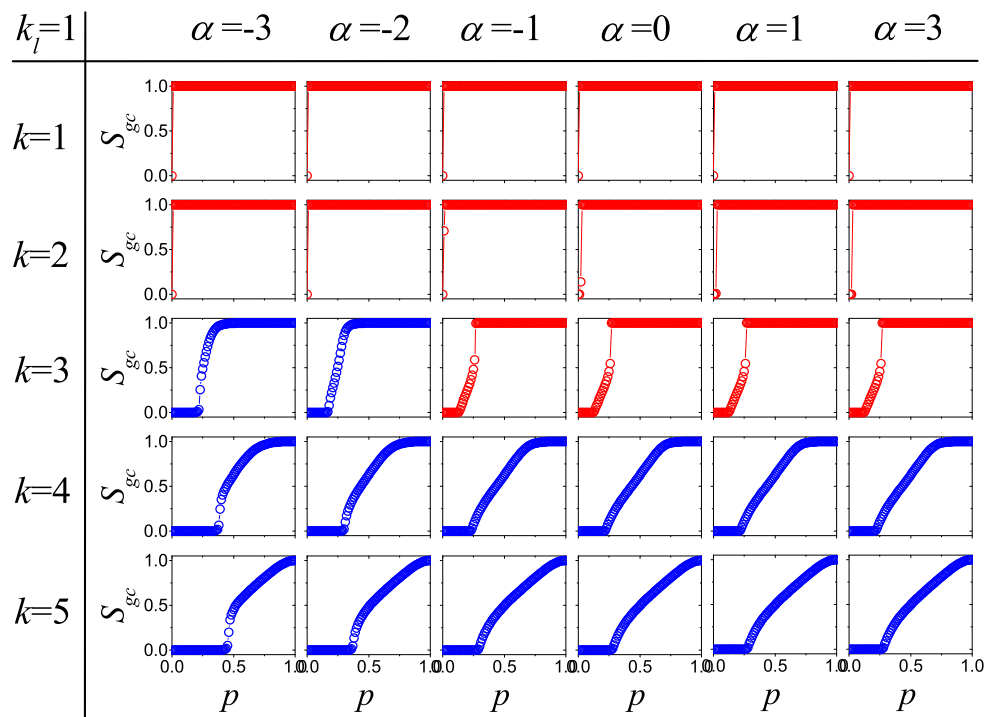


Figure S1. S_{gc} as a function of p after bootstrap percolation on undirected Kleinberg's spatial networks with $k_l = 1$ in parameter spaces (k, α) . Red and blue curves are correspond to the present of a double phase transition (or a first-order phase transition in the trivial cases where $p_{c1} \approx 0$) and a second-order phase transition, respectively. Results are averaged over 1000 realizations with fixed network size $L = 400$.

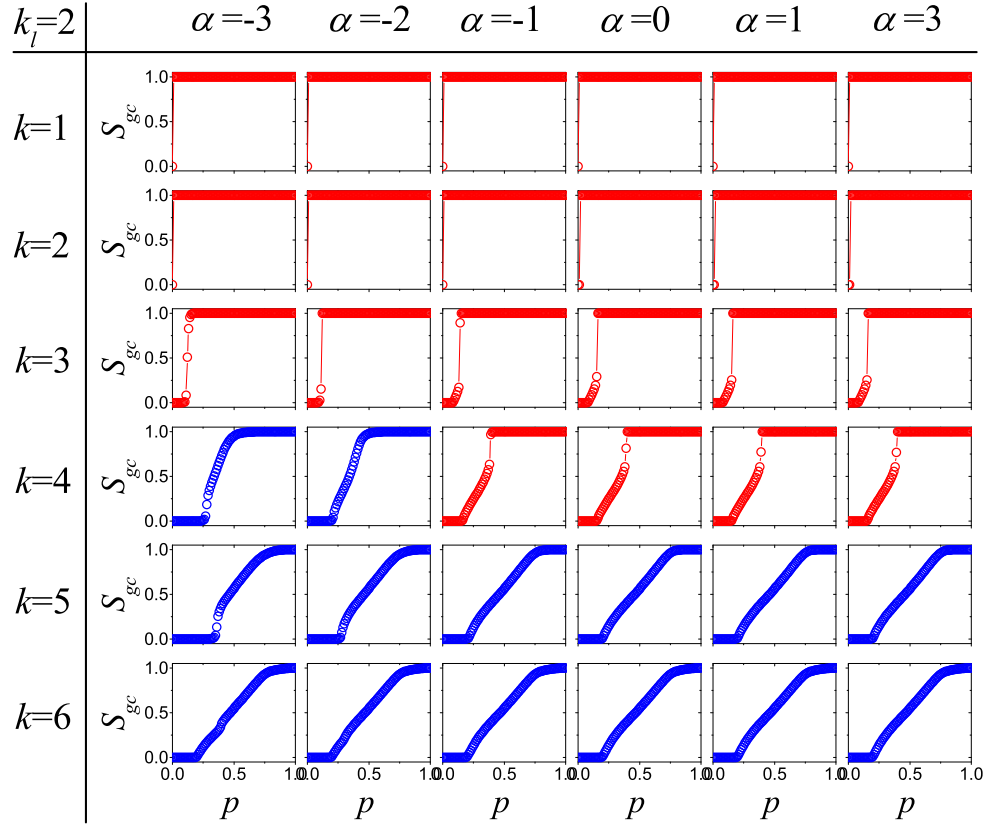


Figure S2. S_{gc} as a function of p after bootstrap percolation on undirected Kleinberg's spatial networks with $k_l = 2$ in parameter spaces (k, α) . Red and blue curves correspond to the presence of a double phase transition (or a first-order phase transition in the trivial cases where $p_{c1} \approx 0$) and a second-order phase transition, respectively. Results are averaged over 1000 realizations with fixed network size $L = 400$.

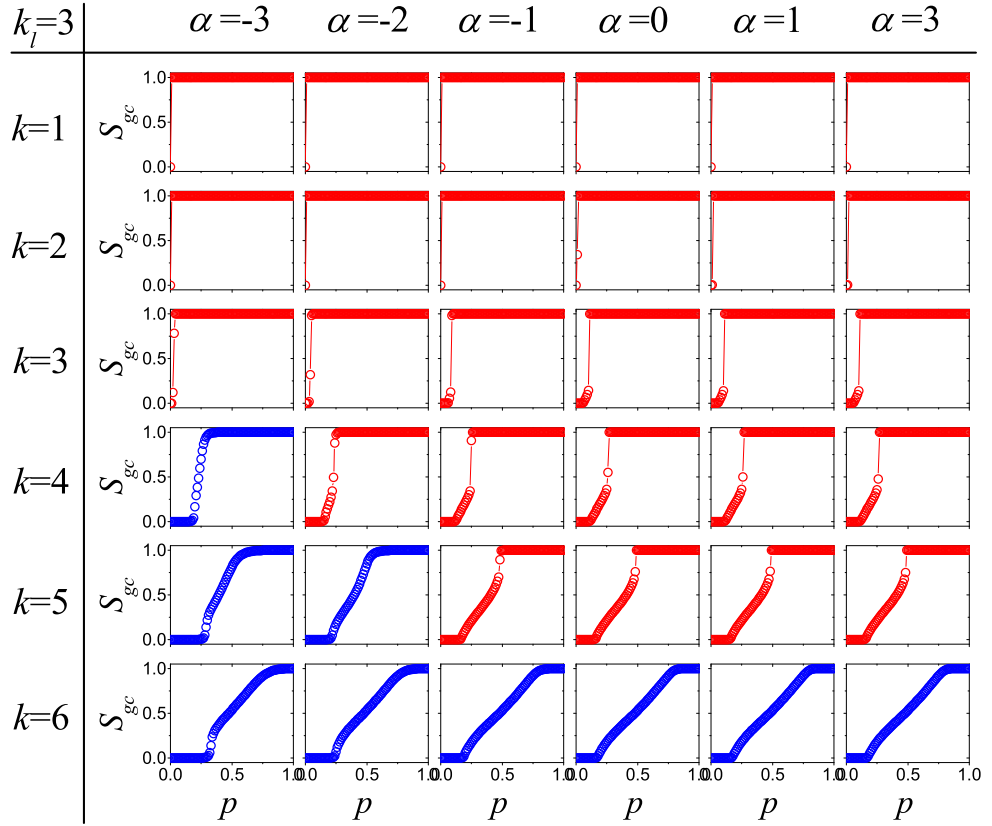


Figure S3. S_{gc} as a function of p after bootstrap percolation on undirected Kleinberg’s spatial networks with $k_l = 3$ in parameter spaces (k, α) . Red and blue curves correspond to the present of a double phase transition (or a first-order phase transition in the trivial cases where $p_{c1} \approx 0$) and a second-order phase transition, respectively. Results are averaged over 1000 realizations with fixed network size $L = 400$.

2. S_{gc} for directed Kleinberg's spatial networks

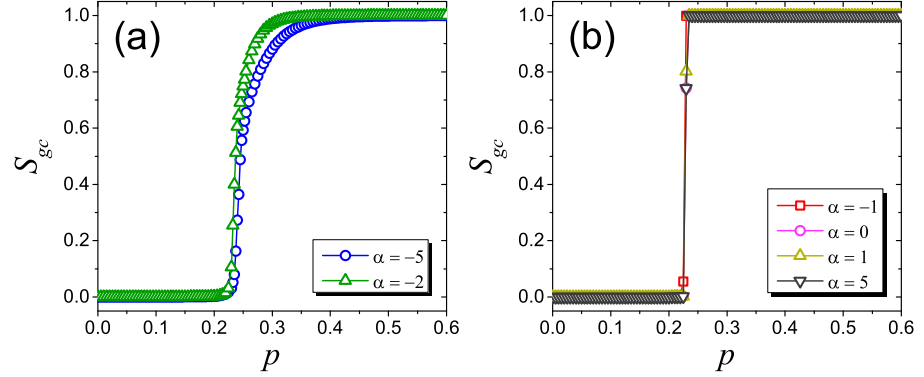


Figure S4. S_{gc} as a function of p after bootstrap percolation on directed Kleinberg's spatial networks in parameter spaces $(k, k_l) = (3, 1)$. Results are averaged over 1000 realizations with fixed network size $L = 400$.

3. Analysis on effects of boundary conditions

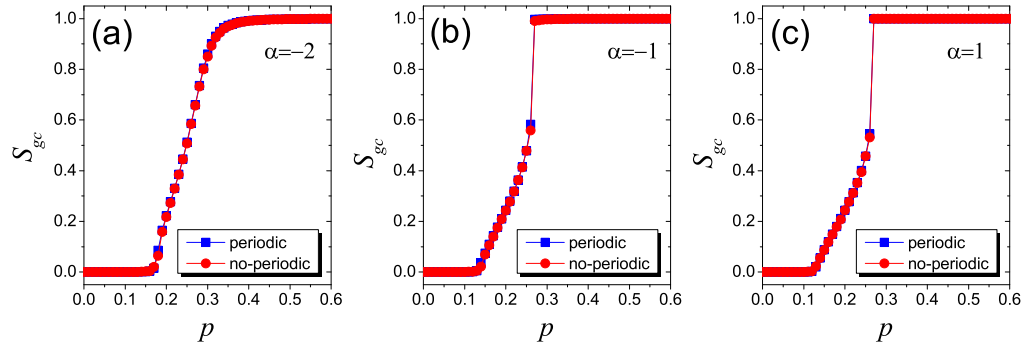


Figure S5. S_{gc} as a function of p after bootstrap percolation on undirected Kleinberg's spatial networks based on square lattice with or without periodic boundary conditions in parameter spaces $(k, k_l) = (3, 1)$. Results are averaged over 1000 realizations with fixed network size $L = 400$.

4. Phase diagram for LR networks

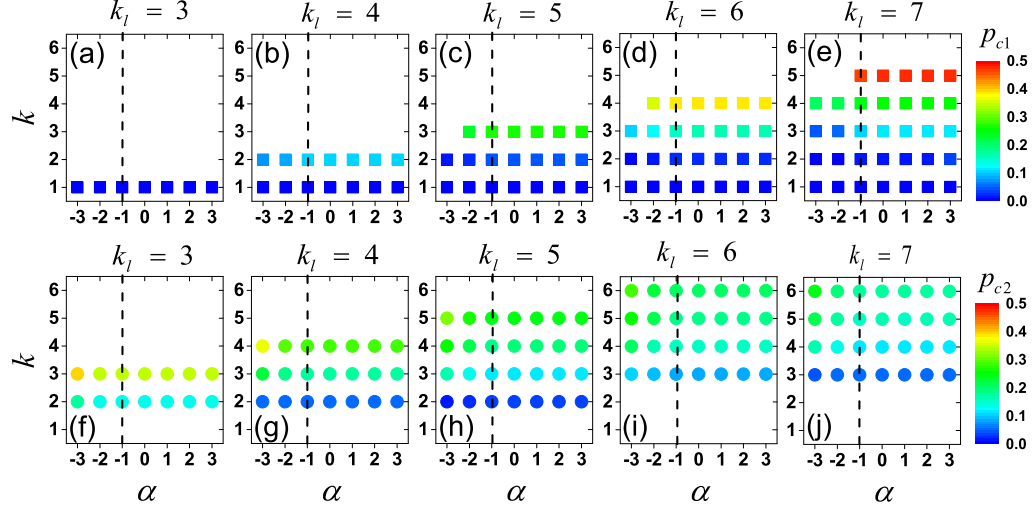


Figure S6. Phase diagram of bootstrap percolation on LR networks in parameter spaces (k , α , k_l). The color of data points in (a), (b), (c), (d) and (e) marks the value of p_{c1} , where there is a hybrid phase transition (or a first-order phase transition in the trivial cases where $p_{c1} \approx 0$), and the color of data points in (f), (g), (h), (i) and (j) marks the value of p_{c2} , where the transition is of second-order. Blank areas stand for the absent of the corresponding phase transitions. Separated by the vertical dash line $\alpha = -1$, on the right side, the color of data points is nearly unchanged for the same parameter k , meaning that the values of p_{c1} and p_{c2} are almost invariant. $\alpha_c \approx -1$ is found to be a robust critical value, above which the critical points for the double phase transition are almost constant. When $\alpha < -1$, p_{c1} decreases and p_{c2} increases as α decreases. Results are averaged over 1000 realizations with fixed network size $L = 400$.

5. S_{gc} for LR networks

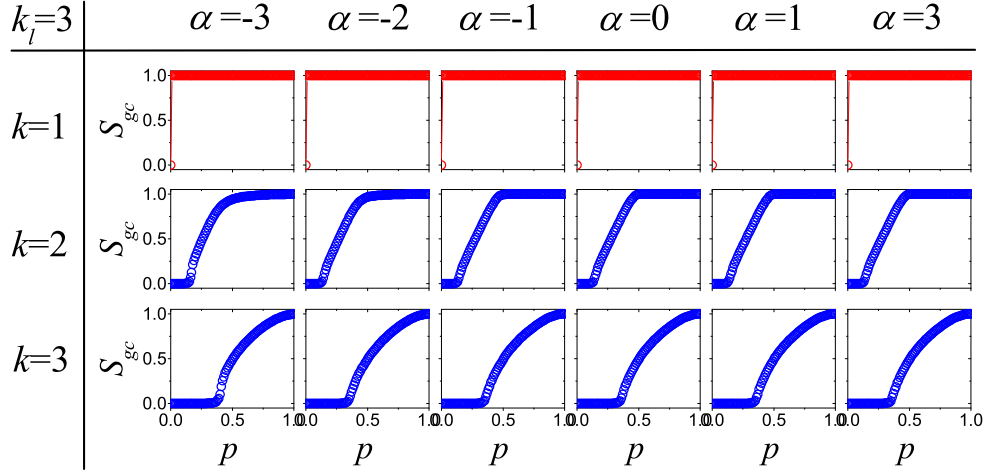


Figure S7. S_{gc} as a function of p after bootstrap percolation on LR networks with $k_l = 3$ in parameter spaces (k, α) . Red and blue curves are correspond to the present of a double phase transition (or a first-order phase transition in the trivial cases where $p_{c1} \approx 0$) and a second-order phase, respectively. Results are averaged over 1000 realizations with fixed network size $L = 400$.

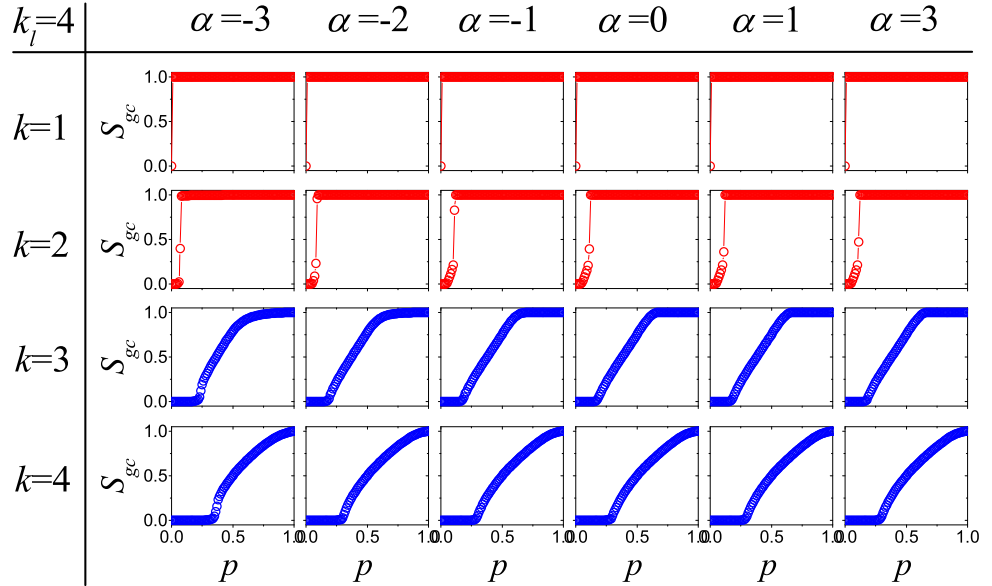


Figure S8. S_{gc} as a function of p after bootstrap percolation on LR networks with $k_l = 4$ in parameter spaces (k, α) . Red and blue curves are correspond to the present of a double phase transition (or a first-order phase transition in the trivial cases where $p_{c1} \approx 0$) and a second-order phase, respectively. Results are averaged over 1000 realizations with fixed network size $L = 400$.

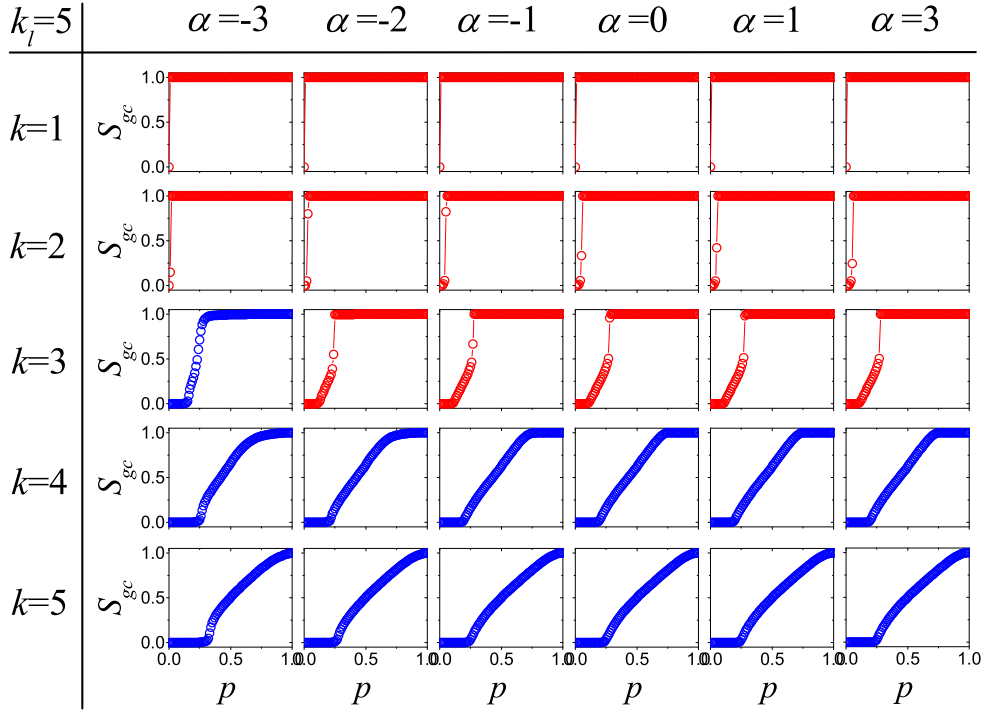


Figure S9. S_{gc} as a function of p after bootstrap percolation on LR networks with $k_l = 5$ in parameter spaces (k, α) . Red and blue curves correspond to the presence of a double phase transition (or a first-order phase transition in the trivial cases where $p_{c1} \approx 0$) and a second-order phase, respectively. Results are averaged over 1000 realizations with fixed network size $L = 400$.

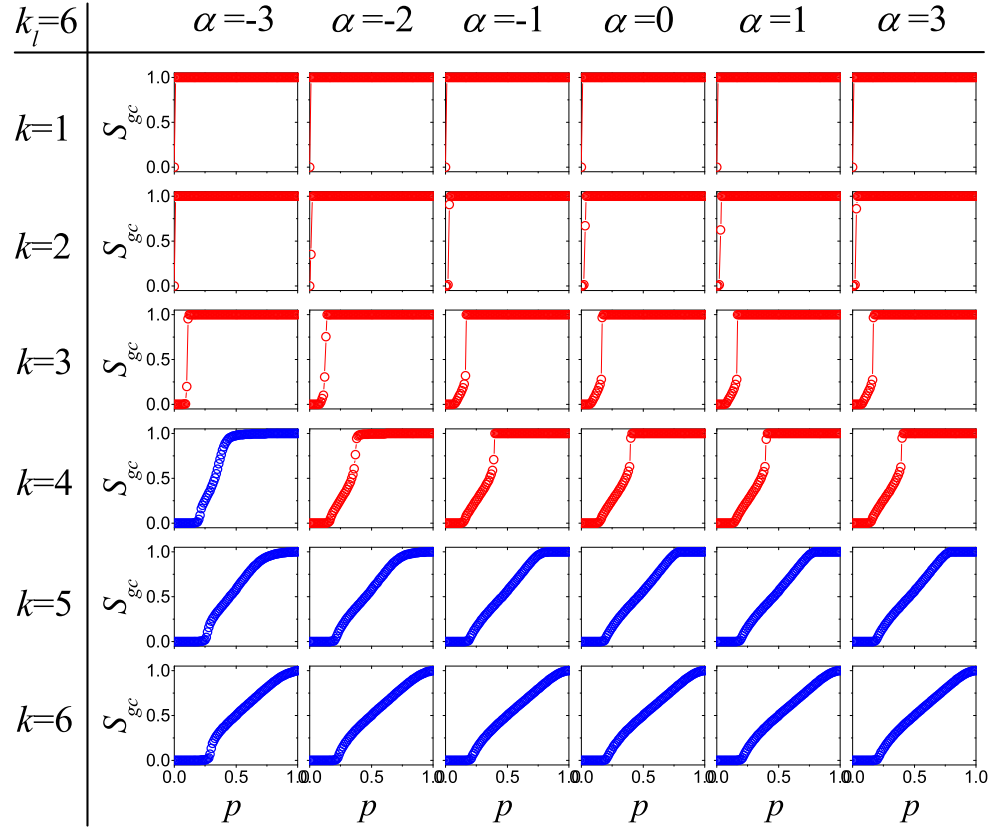


Figure S10. S_{gc} as a function of p after bootstrap percolation on LR networks with $k_l = 6$ in parameter spaces (k, α) . Red and blue curves correspond to the present of a double phase transition (or a first-order phase transition in the trivial cases where $p_{c1} \approx 0$) and a second-order phase, respectively. Results are averaged over 1000 realizations with fixed network size $L = 400$.

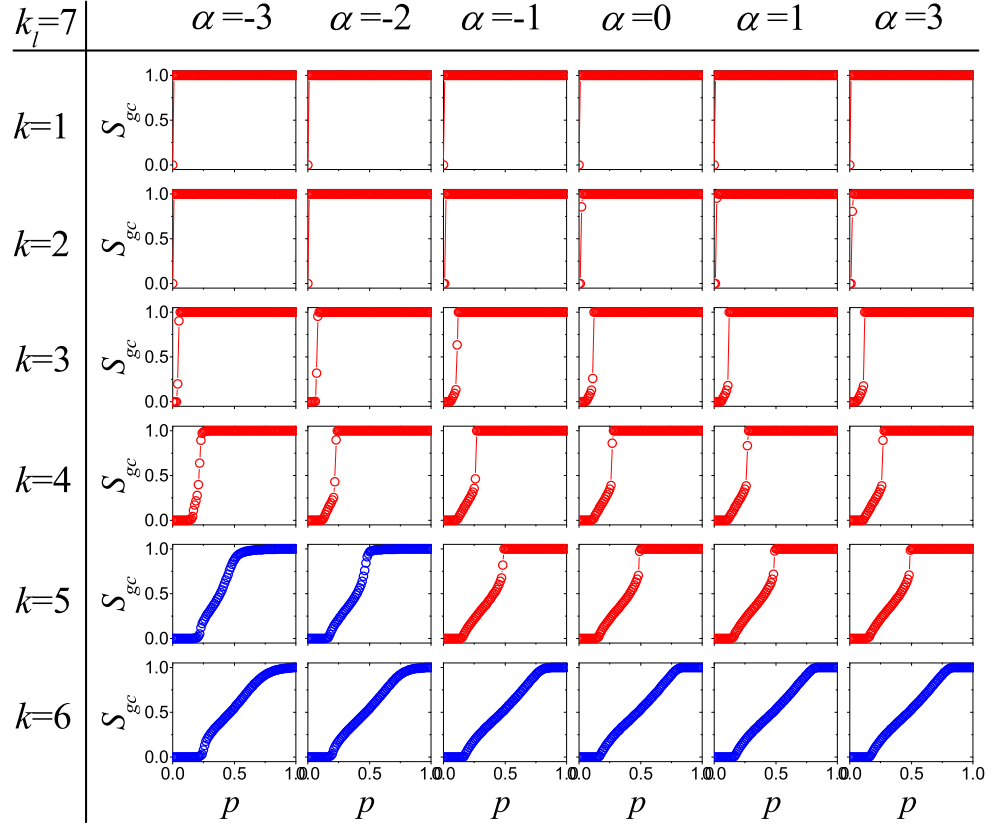


Figure S11. S_{gc} as a function of p after bootstrap percolation on LR networks with $k_l = 7$ in parameter spaces (k, α) . Red and blue curves correspond to the presence of a double phase transition (or a first-order phase transition in the trivial cases where $p_{c1} \approx 0$) and a second-order phase, respectively. Results are averaged over 1000 realizations with fixed network size $L = 400$.